Virginia Polytechnic Institute and State University

The Charles E. Via, Jr.
Department of Civil and Environmental Engineering

CENTER FOR
GEOTECHNICAL PRACTICE AND RESEARCH

ADDENDUM REPORT: A NUMERICAL INVESTIGATION OF THE SEISMIC RESPONSE OF THE AGGREGATE PIER FOUNDATION SYSTEM

by

Morgan A. Eddy
and
Marte S. Gutierrez

Report submitted to the
Geopier Foundation Company, Inc.

February, 2004
Blacksburg, Virginia

List of Tables

List of Figures

Overview

Additional numerical studies were performed to investigate the response of an aggregate pier foundation system during seismic loading. The current study is an extension of an earlier project completed by Girsang and Gutierrez (2001). The goal of the original project was to identify and clarify the factors and phenomena that govern the performance of the aggregate pier and improved ground. The original report identified the matrix soil and aggregate pier densities, stiffness modulus, and drainage capacity as some of these phenomena. The main purpose of the current study is to determine the effect of initial stress conditions and to further investigate the ground acceleration and shear stress in the soil matrix during earthquake loading. This report provides tabulated results, short discussions, and conclusions pertaining to these additional numerical studies. In addition, SHAKE91 site response analyses are performed to illustrate simple methods for performing a site response analysis of aggregate pier reinforced/composite ground.

As with the original work FLAC, a finite difference computer code, was used to perform the two-dimensional dynamic response analyses. The current research was divided into three parts: 1) studies of the ground acceleration, 2) studies of shear stress distribution in the soil matrix generated during dynamic loading, and 3) an example illustrating how an aggregate pier reduces the liquefaction potential of the surrounding soil matrix. The earthquake time histories from the previous study, 1989 Loma Prieta earthquake (pga = 0.45g) and 1988 Saguenay earthquake (pga = 0.05g), were also used in the current study. In the previous study, it appears that the Saguenay earthquake pga was too small to trigger liquefaction. Therefore, both time histories were scaled to values of 0.20g and 0.30g, so that liquefaction would be triggered. To investigate the effects of the initial stress conditions, isotropic stress fields were used in the current study; comparisons were made with the results of the original study, where passive earth pressures were imposed. The isotropic conditions are modeled by setting horizontal stresses equal to vertical stresses.

The six FLAC models used in the current study are shown in Figure 1. The models include: a) unreinforced liquefiable sand (14.5 feet deep), b) unreinforced liquefiable sand (26.5 feet deep), c) unreinforced liquefiable sand underlain by a clay layer (26.5 feet deep), d) reinforced liquefiable sand (14.5 feet deep), e) reinforced liquefiable sand (26.5 feet deep), and f) reinforced liquefiable sand underlain by a clay layer (26.5 feet deep). The original study performed by Girsang and Gutierrez (2001) contains detailed coverage of model dimensions and material properties. The liquefiable silt (26.5 feet deep) model was not used in the current study.

Ground Acceleration

Table 1 contains results of the isotropic FLAC runs, including pga, the maximum horizontal acceleration at the ground surface (a_{max}), the time corresponding to a_{max}, and a note indicating whether amplification or de-amplification occurred. Keeping with the nomenclature of the original study, the cases are identified by a number and letter. The number, ranging from 1 to 6 corresponds to the various models shown in Figure 1, and the letter indicates which earthquake time series was used; C – Loma Prieta and S – Saguenay. The following list indicates the number and corresponding model for the cases contained in Table 1:

1) Unreinforced liquefiable sand (14.5 feet)
2) Reinforced liquefiable sand (14.5 feet)
3) Unreinforced liquefiable sand (26.5 feet)
4) Reinforced liquefiable sand (26.5 feet)
5) Unreinforced liquefiable sand underlain by a clay layer (26.5 feet)
6) Reinforced liquefiable sand underlain by a clay layer (26.5 feet)

Figure 2 contains a plot of amplification ratios based on the soil type compared to relationships proposed by Seed and Idriss (1982); results of the original and current studies are shown for comparison. Keeping in mind that all sites classify as stiff soils per Seed and Idriss (1982), several conclusions can be drawn from Figure 2. 1) When the pga is 0.05g or 0.2g the proposed stiff soil curve roughly splits the data, that is the curve approximately corresponds to the average a_{max}. 2) When the pga is greater than 0.2g the proposed curve overestimates a_{max}. 3) The K_p data points appear to contain more scatter than the isotropic data. Figure 3 contains a plot of amplification ratios based on condition with and without aggregate pier compared to relationships proposed by Seed and Idriss (1982); results of both the original and current studies are shown for comparison. Figure 3 shows several general trends. 1) For a pga of 0.05g the proposed stiff soil curve falls in the middle of the data. 2) For a pga of 0.2g, "with pier" data points tend to fall above the proposed curve while "no pier" data points typically fall below the curve. 3) For a pga of 0.3g and 0.45g, the data falls below the proposed one-to-one curve.

SHAKE91 runs were performed to determine whether composite material properties could be used to estimate FLAC results. The sand damping and shear modulus degradation curves given in the SHAKE91 User's Manual (1971) were used for both the unreinforced and composite materials. Equation 1 (after Baez and Martin, 1993, 1994) was used to compute composite material properties to be used in SHAKE91.

$$X = \frac{(X_g * A_g + X_s * A_s)}{A} \qquad \text{(EQ. 1)}$$

where: X = composite material property
X_g = pier material property
X_s = soil matrix material property
A_g = area of pier
A_s = area of soil matrix
A = total area

All cases analyzed with FLAC, both unreinforced and reinforced (composite), were modeled with SHAKE91. Table 2 contains results of the SHAKE91 runs including pga, a_{max}, and the time at which a_{max} occurs. Table 2 indicates that all models de-amplified the pga except for models where the aggregate pier extends to the rock surface. Non-realistic results occur when the aggregate pier/soil matrix is modeled as a composite layer atop a softer layer. Figures 4 and 5 contain plots of the SHAKE91 results illustrating the amplification ratio, similar to Figures 2 and 3. Figure 4 shows that silty sand models fell just below the recommended stiff soil line and the silty sand atop soft clay models fell below the soft to medium stiff clay and sand line as proposed by Seed and Idriss (1982). Figure 5 shows four models containing the composite layer, representing the aggregate

pier/soil matrix materials, where amplification occurred. These sites correspond to the models where the aggregate pier extends to the rock surface.

Shear Stress in Soil Matrix

In the original study, results for the liquefiable sand (14.5 feet) were presented and discussed in detail. For consistency and easy comparison, results for the liquefiable sand (14.5 feet) are also presented in this study. Figure 6 shows the change in shear stress (τ_s) between the unreinforced (1C) and reinforced (2C) models; both passive (K_p) and isotropic initial stress conditions are shown. In both the K_p and isotropic cases, it is clear that the aggregate pier carries more shear stress than the surrounding soils. The K_p situation contains considerable scatter and non-uniformity as compared to the isotropic case, possibly associated with unrealistic soil failure.

Figure 7 contains plots of the shear stress reduction factor (K_G) for both the K_p and isotropic stress conditions. Figure 7 indicates several points of consideration: 1) For the K_p situation, the shear stress in the soils determined by FLAC is typically less than half of the shear stress computed by the Simplified Procedure (Seed and Idriss, 1971). 2) For the K_p case, the shear stress in the aggregate pier is greater than the Simplified Procedure for depths less than 3.25 feet and less than the Simplified Procedure for depths greater than or equal to 3.25 feet. 3) For isotropic conditions, the shear stress in the soil is less than the Simplified Procedure for depths greater than or equal to 7.75 feet (including a depth of 0.25 feet) and greater than the Simplified Procedure for depths less than 7.75 feet (excluding a depth of 0.25 feet). 4) For the isotropic case, the shear stress in the aggregate pier is greater than the Simplified Procedure for depths greater than or equal to 7.75 feet (including a depth of 0.25 feet) and less than the Simplified Procedure for depths less than 7.75 feet (excluding a depth of 0.25 feet).

Figure 8 contains plots of the reinforcement factor (K_{GR}) for both the K_p and isotropic stress conditions for the liquefiable sand (14.5 feet) model. Comparing the two plots indicates that the initial stress conditions impact the K_{GR} value. For the K_p situation, the maximum shear stress in the aggregate pier are between ½ to 20 times that of the unreinforced soil, whereas in isotropic case, the τ_{max} is only ½ to 2 times that of the unreinforced soil. The large difference is most likely a result of unrealistic soil failure under K_p conditions.

Figure 9 contains a comparison of K_G and K_{GR} values in the soil matrix and the aggregate pier for the liquefiable sand (14.5 feet) model; both K_p and isotropic initial stress conditions are shown. Figure 9 shows that the correlation between K_{GR} and K_G for the K_p situation contains significant scatter, however a general trend is observed where a large change in K_{GR} results in a small K_G change. For the isotropic case, the plotted K_{GR} and K_G values indicate an approximate one-to-one relationship, with limited scatter.

To compare the results of the FLAC and SHAKE91 analyses, the FLAC results were manipulated so as to obtain a composite shear stress. This process was executed by using equation 1, where average maximum shear stresses in the soil matrix and aggregate pier are input. Figure 10 contains plots of the composite maximum shear stress versus depth for both the SHAKE91 and FLAC analyses, the profiles are in general agreement.

Simplified Procedure for Evaluating Liquefaction Potential of Aggregate Pier Foundation System

Site response analyses with advanced computer software such as FLAC is rarely justified for small to medium projects where aggregate piers may be used; therefore a simple procedure is needed to account for reinforcing elements. Based on the results of this and other studies (including Baez and Martin, 1993, 1994 and Gutierrez and Girsang, 2001) on the aggregate pier foundation system, a simplified procedure is outlined as follows:

1. Determine the pga for the site of interest. The pga can be obtained from attenuation relationships or seismic hazard maps.
2. Determine the K_G or K_{GR} value. The K_G value can be estimated using Figure 11 (from Baez and Martin. 1993, 1994) based on the area replacement ratio, R_A and the shear modulus ratio, R_s. The K_{GR} value is equal to the K_G value based on isotropic stress conditions, and larger than K_G for stress conditions approaching passive.
3. Compute the composite shear modulus or shear wave velocity and composite unit weight using equation 1.
4. Use NEHRP provisions, SHAKE91, or amplification relationships such as those proposed by Seed and Idriss (1982) to estimate a_{max}.
5. Determine the non-composite and composite CSR or τ_{max} using the Simplified Procedure (Youd et al., 2001).
6. Determine the CSR and τ_{max} in the soil matrix and aggregate pier with the value of K_{GR}.

The procedure described above is illustrated with the following example. Figure 11 contains the basic geometry of the example problem containing liquefiable silty sand; the depth into the page is equal to the width of the model (8.4 feet). Table 3 contains material properties and areas of the soil matrix and aggregate pier used in the example problem. The shear wave velocity of the rock is assumed to be 5000 fps.

1. Assume the pga for the example is 0.20g
2. $$R_A = \frac{A_r}{A} = \frac{7.07\text{ft}^2}{70.56\text{ft}^2} = 0.1$$

   $$R_s = \frac{G_r}{G_s} = \frac{968000\text{psf}}{121000\text{psf}} = 7$$

   From Figure 11, K_G is approximately equal to 0.63.
3. $$V_{scomposite} = \frac{(63.49\text{ft}^2 * 180\text{fps}) + (7.07\text{ft}^2 * 460\text{fps})}{70.56\text{ft}^2} = 208\text{fps}$$

   $$\gamma_{satcomposite} = \frac{(63.49\text{ft}^2 * 120\text{pcf}) + (7.07\text{ft}^2 * 147\text{pcf})}{70.56\text{ft}^2} = 122.71\text{pcf}$$
4. Using the recent NEHRP provisions, the site classification is based on the average shear wave velocity in the top 100 feet of the site. Including the rock below the silty sand, the site would classify as a Site Class B, therefore the short period site amplification factor, F_A, is equal to 1.0 or the a_{max} is equal to the pga.

5. The CSR is calculated at a depth of 7.0 feet (this procedure is discussed by Girsang and Gutierrez, 2001).

$\sigma_o = (120pcf) * (7.0ft) = 840psf$

$\sigma_{o-composite} = (122.71pcf) * (7.0ft) = 859psf$

$\sigma'_o = (120pcf - 62.4pcf) * (7.0ft) = 403psf$

$\sigma'_{o-composite} = (122.71pcf - 62.4pcf) * (7.0ft) = 422psf$

$r_d = 1 - 0.00765(7.0feet / 3.28meters / foot) = 0.984$

$$CSR = 0.65 * \frac{\sigma_o}{\sigma'_o} * \frac{a_{max}}{g} r_d = 0.65 * \frac{840psf}{403psf} * \frac{0.2g}{g}(0.984) = 0.267$$

$$CSR_{composite} = 0.65 * \frac{859psf}{422psf} * \frac{0.2g}{g}(0.984) = 0.260$$

$$CSR_{composite} = \frac{(63.49ft^2 * CSR_{soil}) + (7.07ft^2 * CSR_{pier})}{70.56ft^2} = 0.260$$

6. $K_G = K_{GR} = 0.63$ therefore $CSR_{soil} = 0.63CSR_{pier}$

$$0.260 = \frac{(63.49ft^2 * 0.63CSR_{pier}) + (7.07ft^2 * CSR_{pier})}{70.56ft^2}$$

$CSR_{pier} = 0.390$

$CSR_{soil} = 0.246$

This example shows how the aggregate pier reduces the CSR in the surrounding soil matrix, therefore reducing the liquefaction potential of the silty sand. The CSR of the soil matrix without the aggregate pier is estimated as 0.267, whereas the CSR of the soil matrix with the aggregate pier is approximately 0.246.

Conclusions

Results from additional numerical studies of the seismic response of the aggregate pier foundation system were presented. The additional studies, performed with FLAC, aimed to refine the results of the original study performed by Girsang and Gutierrez (2001). The current study used the original time histories from the 1989 Loma Prieta earthquake and the 1988 Saguenay earthquake scaled to 0.2g and 0.3g. It should be noted that scaling the low acceleration Saguenay record by a factor of six may lead to unrealistic results. Conclusions drawn from this study are similar to the original study. In terms of amplification, the a_{max} of the aggregate pier system tends to be amplified for pga's of 0.05g and 0.2g; whereas the a_{max} is de-amplified for pga's of 0.3g and 0.45g. Under seismic loading, the aggregate pier typically carries higher shear stresses than the surrounding soil, effectively reducing liquefaction potential. The K_G of the aggregate piers tends to be greater than one; with soil matrix K_G values typically one-half to one. The K_{GR} factor is the limit for the K_G value; however the K_G value is typically less than K_{GR}. An example problem was provided, illustrating a simplified procedure for estimating the reduction in liquefaction potential associated with the aggregate pier foundation system.

Future investigators of the seismic response of the aggregate pier foundation system should consider the following:

1) Perform detailed parametric studies of each individual case to gain a better understanding of the dynamic interplay between the aggregate pier and the surrounding liquefiable soil.
2) Simulations with a broader range of un-scaled earthquake time series used to trigger liquefaction should be used to investigate the effect of different earthquake parameters including duration, magnitude, epicentral distance, and frequency content.
3) Additional values of pga should be implemented to gain a fundamental understanding of the amplification behavior of the aggregate pier foundation system.

References

Baez, J. I. and Martin, G. R. (1993). "Advances in the Design of Vibro Systems for the Improvement of Liquefaction Resistance", *Proceedings of the 7th Annual Symposium of Ground Improvement*, 1-16.

Baez, J. I. and Martin, G. R. (1994). "Advances in the Design of Vibro Systems for the Improvement of Liquefaction Resistance", *The 2nd Seismic Short Course on Evaluation and Mitigation of Earthquake Induced Liquefaction Hazards*, Division of Engineering San Francisco State University and Department of Civil Engineering University of Southern California, 1-16.

FLAC User's Manual – version 4.0. (2000). Itasca Consulting Group, Inc., Minneapolis, Minnesota.

Girsang, C.H. and Gutierrez, M.S. (2001). "A Numerical Investigation of the Seismic Response of the Aggregate Foundation System", Virginia Polytechnic Institute and State University, 192pp.

Idriss, I. M. and Sun, J. I. (1992). "SHAKE91: A Computer Program for Conducting Equivalent Linear Seismic Response Analyses of Horizontally Layered Soil Deposits", University of California, Davis, California, 13pp.

Seed, H.B. and Idriss, I.M. (1971). "Simplified Procedure for Evaluating Soil Liquefaction Potential", *Journal of Soil Mechanics & Foundations Division*, ASCE 97(SM9), 1249-1273.

Seed, H.B. and Idriss, I.M. (1982). "Ground Motions and Soil Liquefaction during Earthquakes", Earthquake Engineering Research Institute, 134pp.

Youd, T. L., Idriss, I. M., Andrus, R. D., Arango, I., Castro, G., Christian, J. T., Dobry, R., Finn, W. D. L., Harder, L. F., Hynes, M. E., Ishihara, K., Koester, J. P., Liao, S. S. C., Marcuson, W. F., Martin, G. R., Mitchell, J. K., Moriwaki, Y., Power, M. S., Robertson, P. K., Seed, R. B., and Stokoe, K. H. (2001). "Liquefaction Resistance of Soils: Summary Report from the 1996 NCEER and 1998 NCEER/NSF Workshops on Evaluation of Liquefaction Resistance of Soils", *Journal of Geotechnical and Geoenvironmental Engineering*, ASCE, 127(10), 817-833.

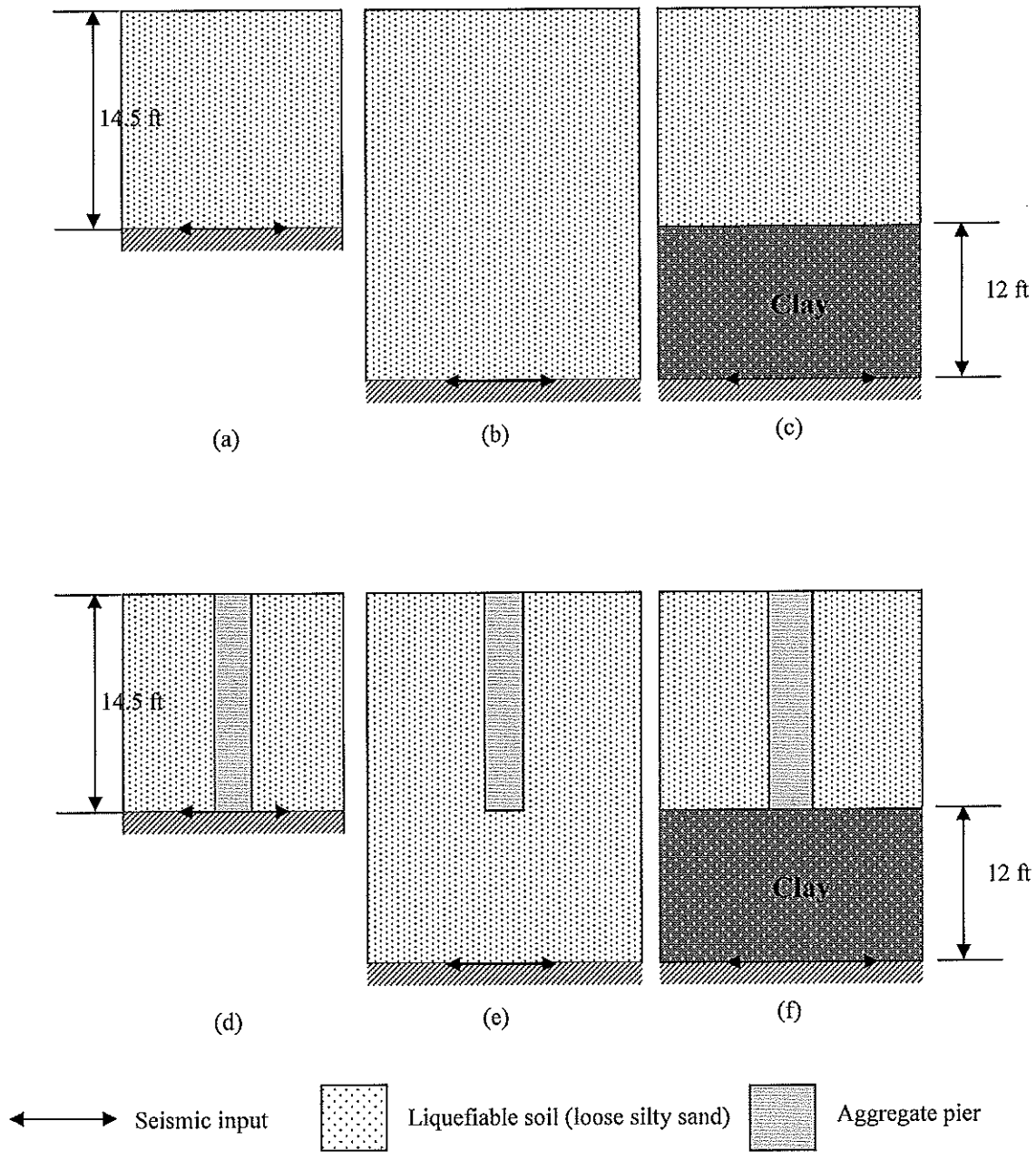

Figure 1 – Models used in isotropic initial conditions FLAC runs.

Table 1 – Acceleration (pga and a_{max}) values from isotropic FLAC runs.

Case	pga	Soil		Note	Pier		Note
		a_{max}	time, sec		a_{max}	time, sec	
1C	0.20	0.21	0.58	Amplification	-	-	-
1C	0.30	0.21	0.56	De-amplification	-	-	-
2C	0.20	0.21	0.61	Amplification	0.21	0.59	Amplification
2C	0.30	0.24	0.56	De-amplification	0.22	0.94	De-amplification
3C	0.20	0.22	0.67	Amplification	-	-	-
3C	0.30	0.22	0.63	De-amplification	-	-	-
4C	0.20	0.29	0.68	Amplification	0.28	1.04	Amplification
4C	0.30	0.18	0.63	De-amplification	0.25	0.81	De-amplification
5C	0.20	0.17	0.81	De-amplification	-	-	-
5C	0.30	0.21	0.71	De-amplification	-	-	-
6C	0.20	0.20	0.74	Same	0.23	0.95	Amplification
6C	0.30	0.23	0.70	De-amplification	0.25	0.72	De-amplification
1S	0.20	0.13	0.93	De-amplification	-	-	-
1S	0.30	0.13	0.93	De-amplification	-	-	-
2S	0.20	0.12	0.94	De-amplification	0.13	0.93	De-amplification
2S	0.30	0.15	0.93	De-amplification	0.17	0.94	De-amplification
3S	0.20	0.10	1.02	De-amplification	-	-	-
3S	0.30	0.15	1.00	De-amplification	-	-	-
4S	0.20	0.10	1.01	De-amplification	0.20	1.97	Same
4S	0.30	0.12	1.01	De-amplification	0.24	2.21	De-amplification

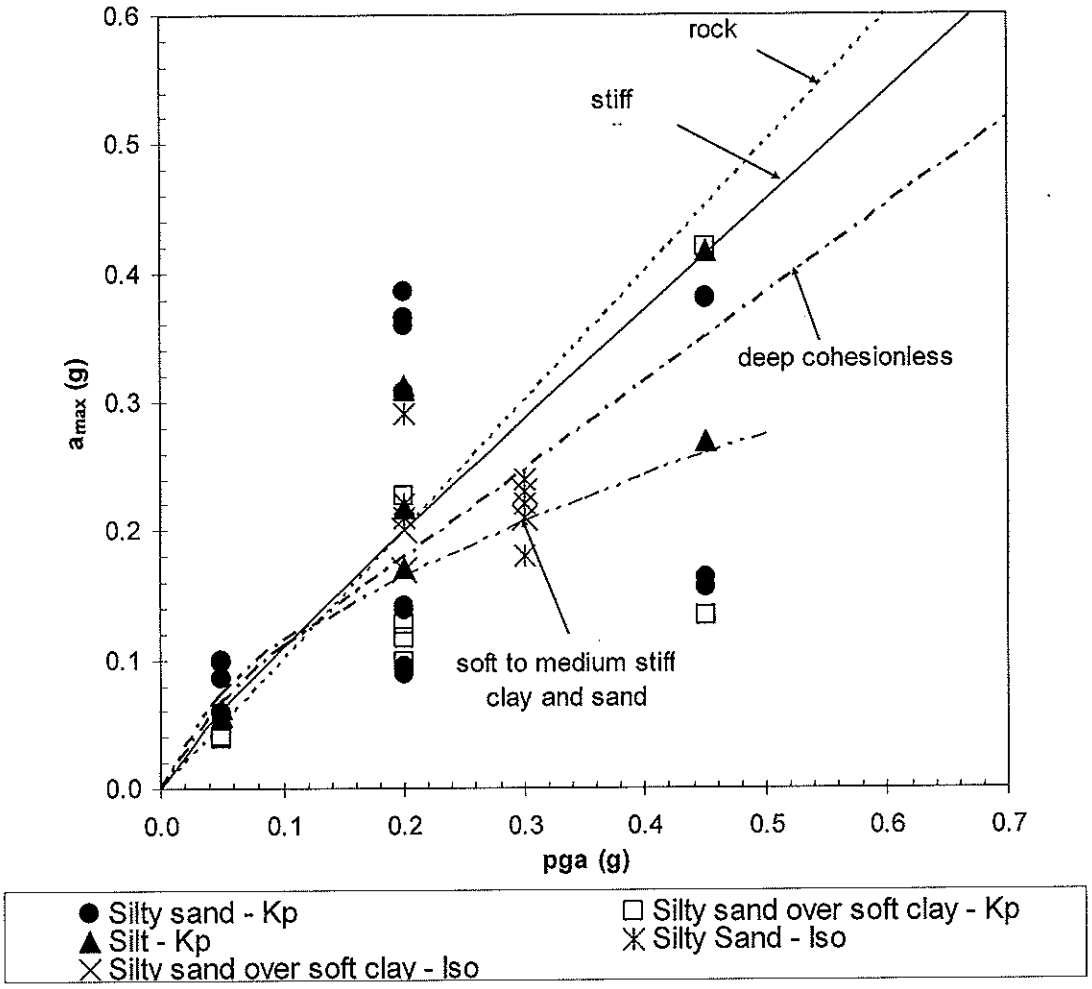

Figure 2 - Plot of amplification ratios (FLAC) based on the soil type compared to those proposed by Seed and Idriss (1982).

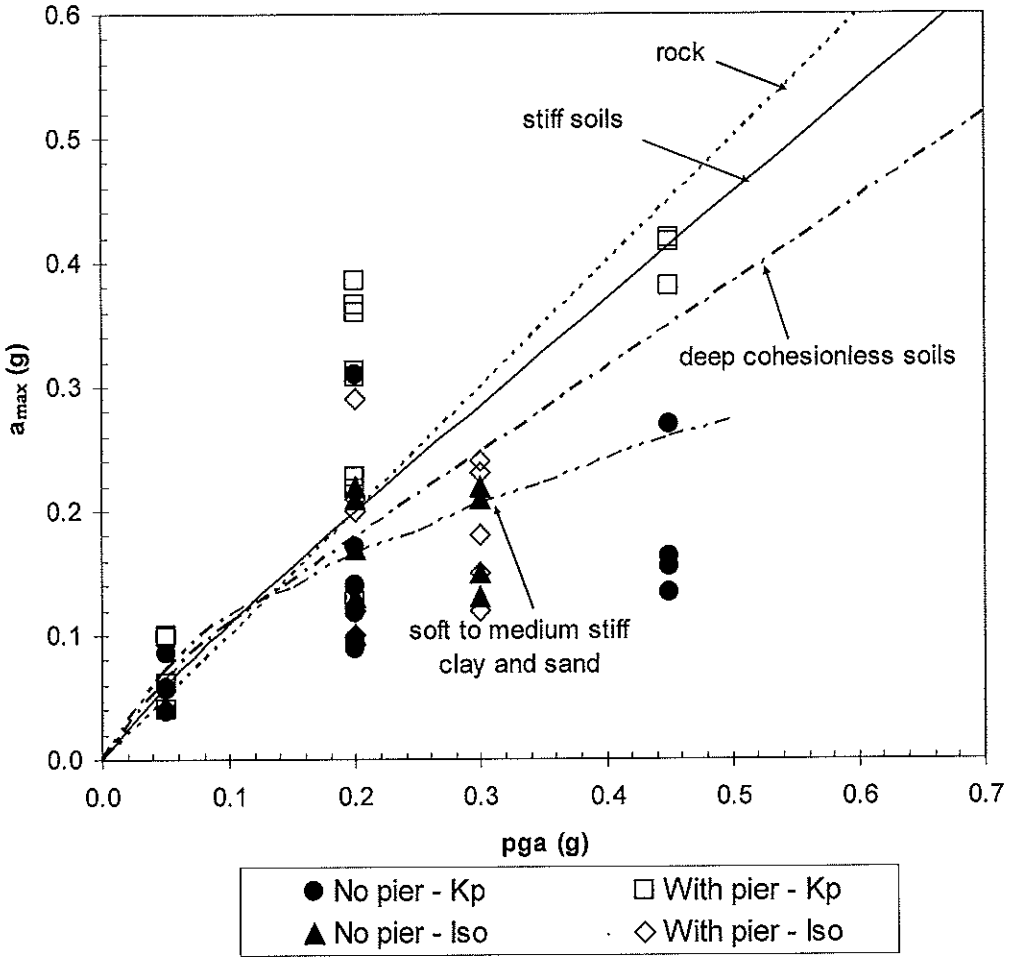

Figure 3 - Plot of amplification ratios (FLAC) based on condition with and without aggregate pier compared to those prepared by Seed and Idriss (1982).

Table 2 - Acceleration (pga and a_{max}) values from SHAKE91 runs.

Case	pga	a_{max}	time, sec	Note
1C	0.20	0.21	1.34	Amplification
1C	0.30	0.23	1.37	De-amplification
2C	0.20	0.26	0.91	Amplification
2C	0.30	0.33	0.92	Amplification
3C	0.20	0.16	1.04	De-amplification
3C	0.30	0.20	1.09	De-amplification
4C	0.20	0.10	1.00	De-amplification
4C	0.30	0.14	1.02	De-amplification
5C	0.20	0.12	1.05	De-amplification
5C	0.30	0.17	1.09	De-amplification
6C	0.20	0.08	1.01	De-amplification
6C	0.30	0.12	1.03	De-amplification
1S	0.20	0.19	2.73	De-amplification
1S	0.30	0.26	2.74	De-amplification
2S	0.20	0.25	2.11	Amplification
2S	0.30	0.29	3.46	De-amplification
3S	0.20	0.18	2.22	De-amplification
3S	0.30	0.20	2.23	De-amplification
4S	0.20	0.13	2.19	De-amplification
4S	0.30	0.18	2.20	De-amplification

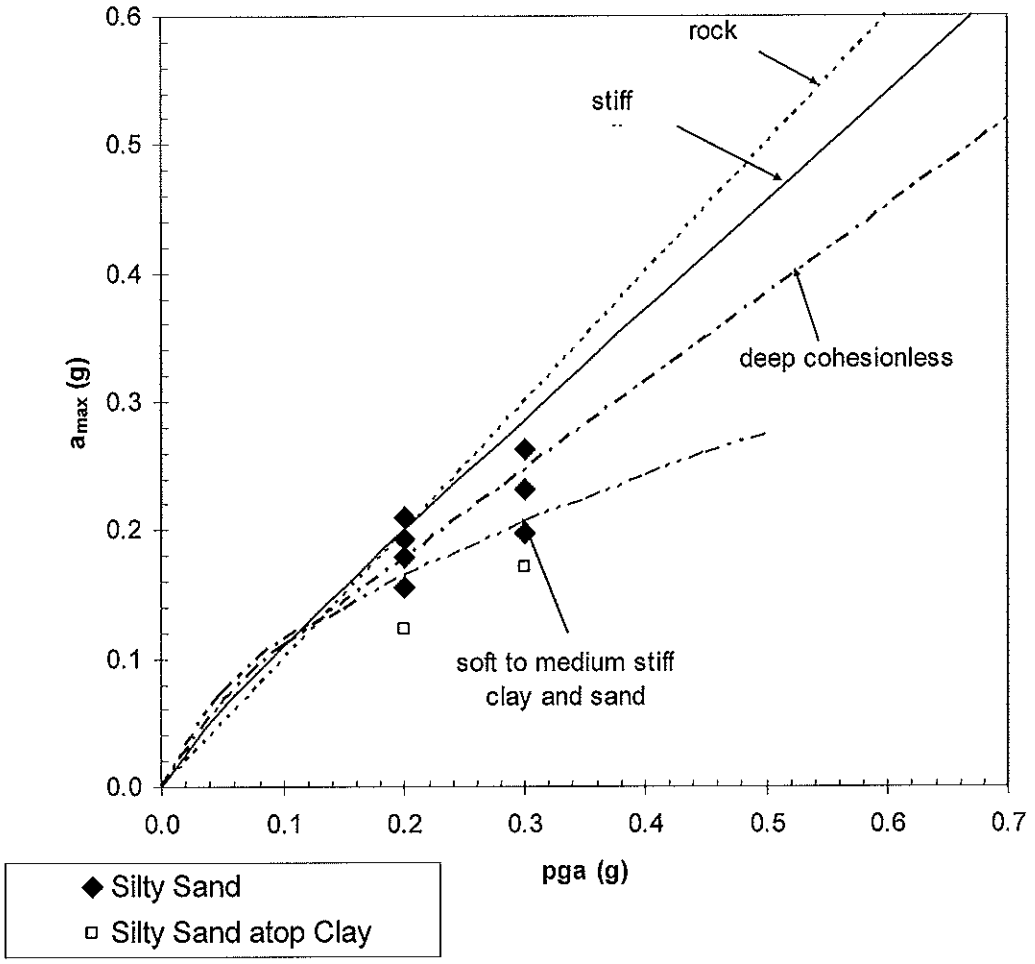

Figure 4 - Plot of amplification ratios (SHAKE91) based on the soil type compared to those proposed by Seed and Idriss (1982).

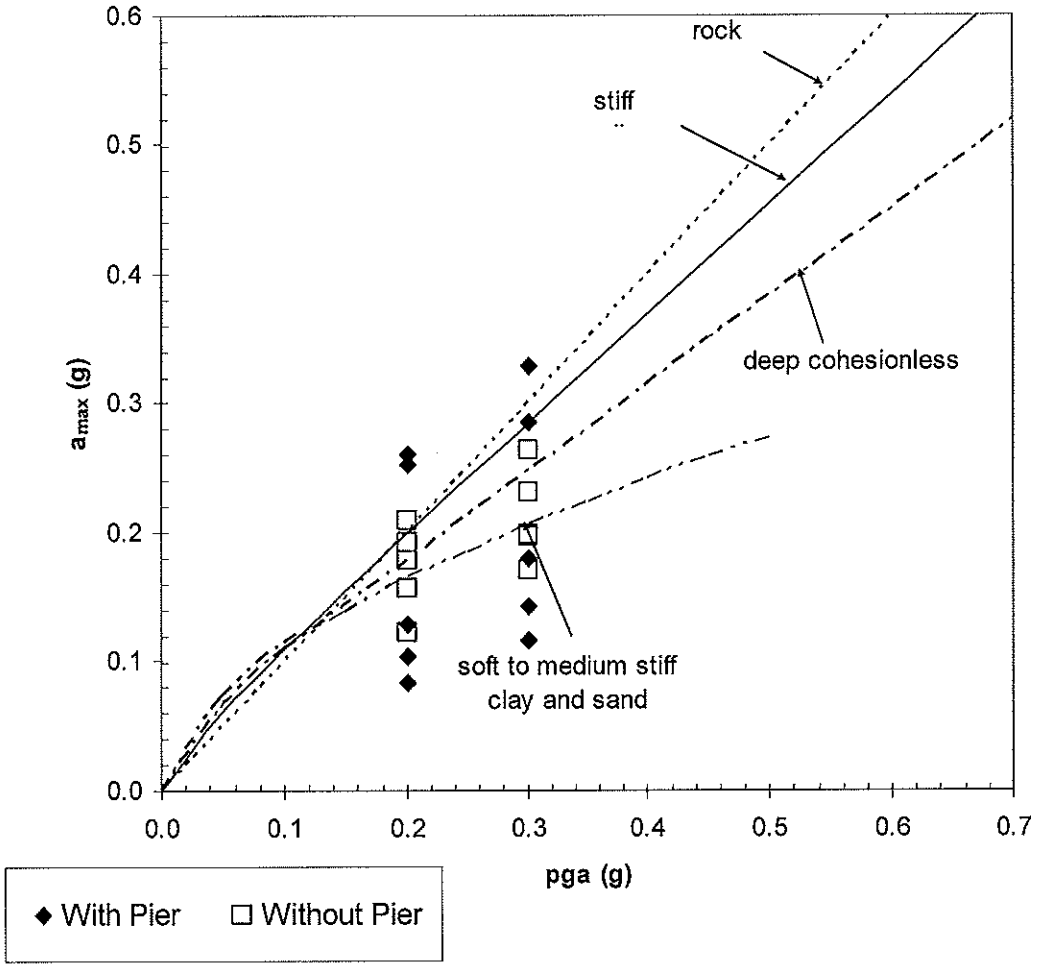

Figure 5 - Plot of amplification ratios (SHAKE91) based on condition with and without aggregate pier compared to those prepared by Seed and Idriss (1982).

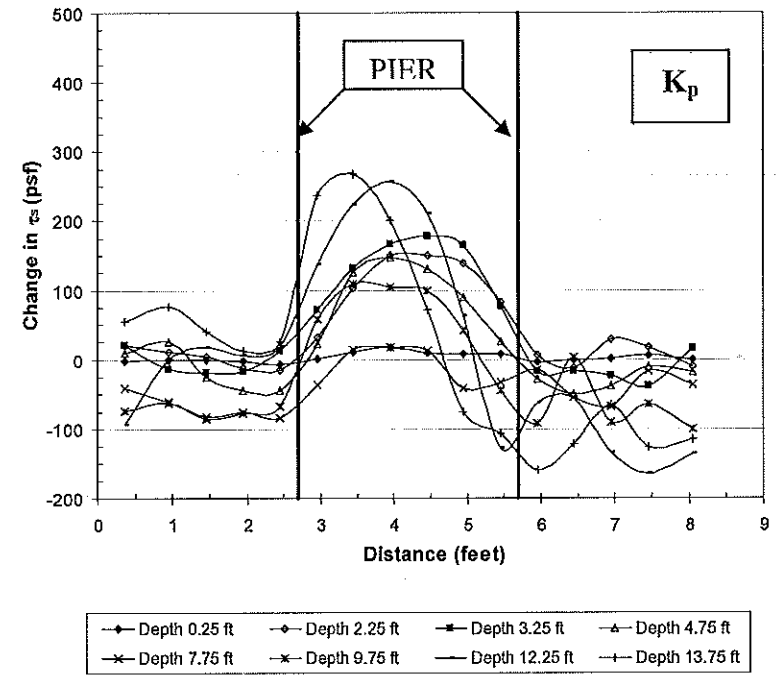

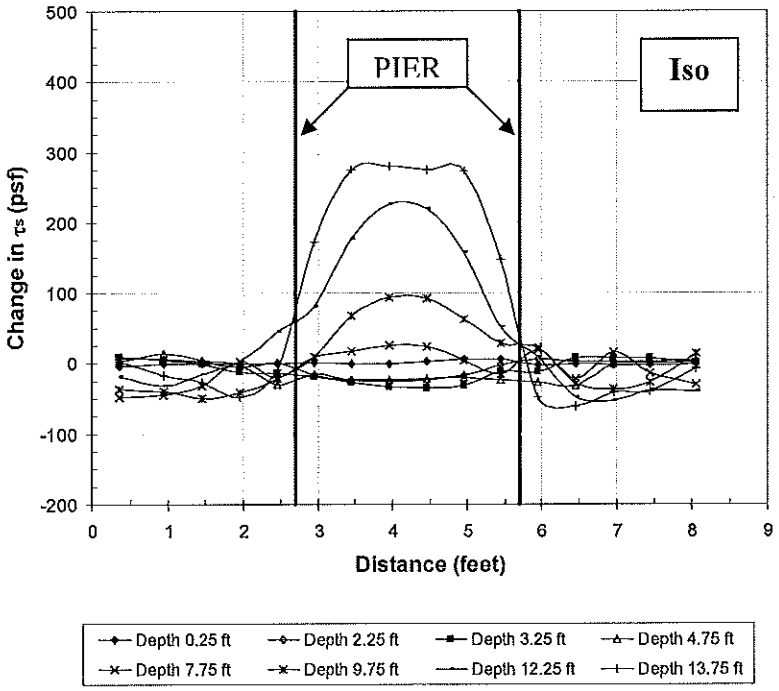

Figure 6 - Change in τ_s between unreinforced (1C2) and reinforced (2C2) FLAC runs; K_p initial conditions (top), isotropic initial conditions (bottom).

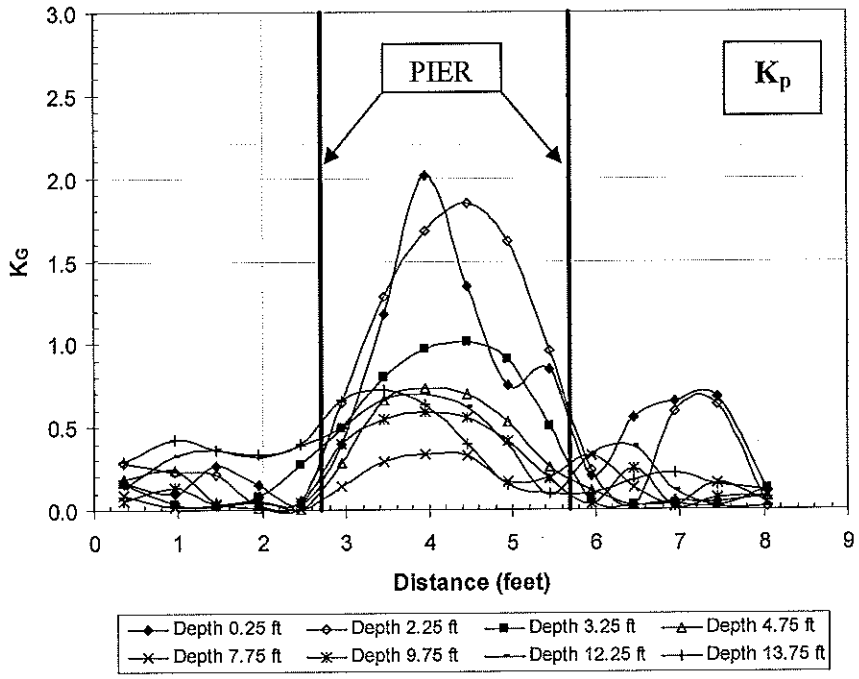

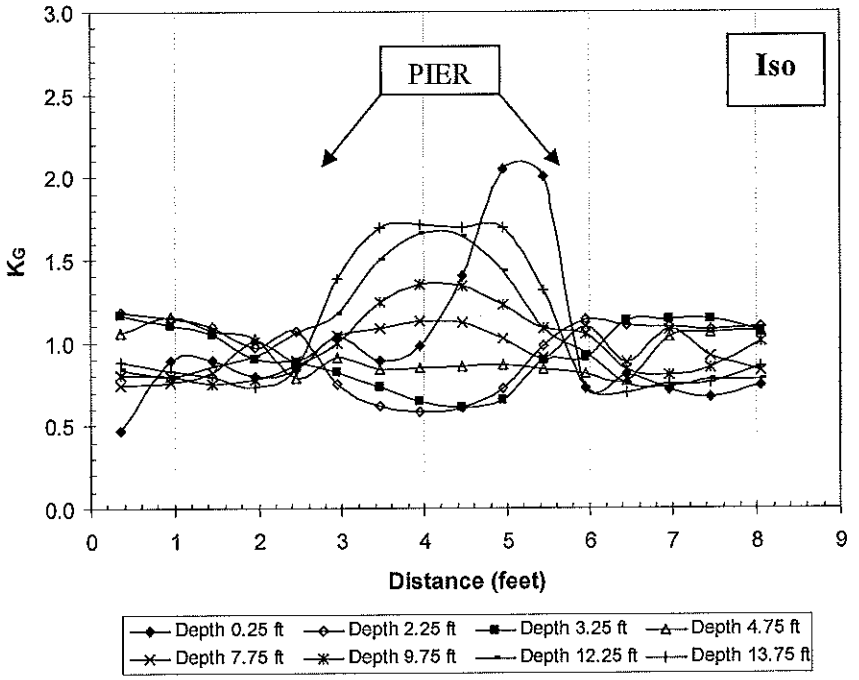

Figure 7 - Plots of values of K_G versus distance for different depths for Case 2C2; K_p initial conditions (top), isotropic initial conditions (bottom).

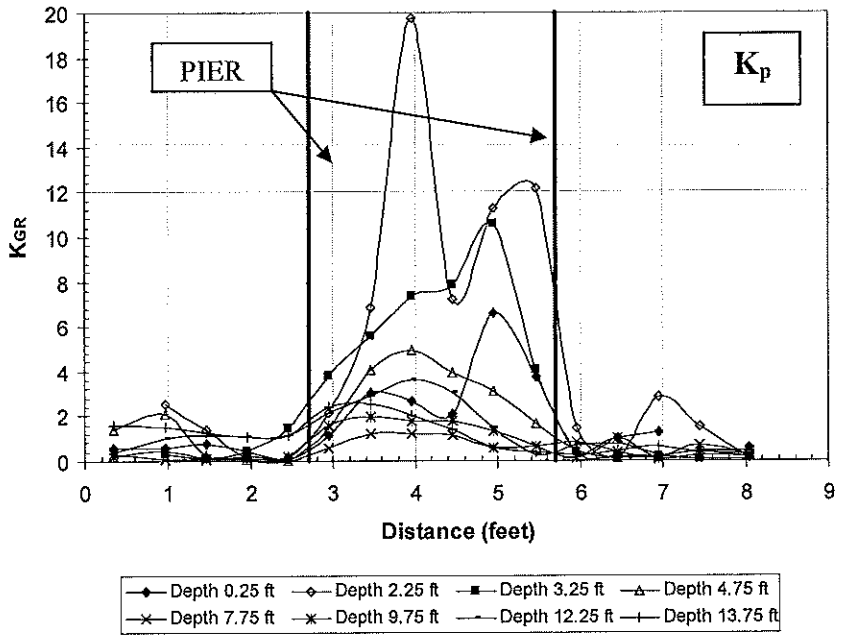

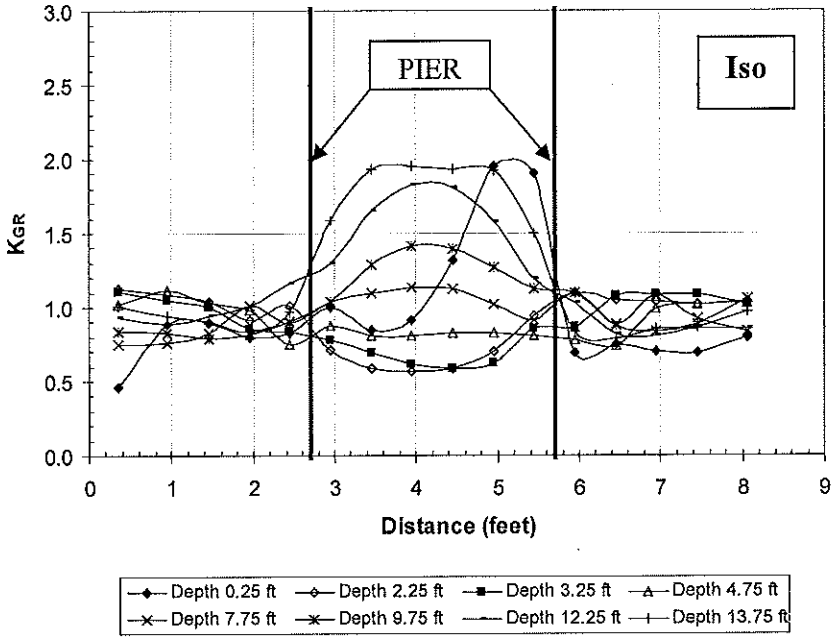

Figure 8 - Plots of values of K_{GR} versus distance for different depths for Case C2; K_p initial conditions (top), isotropic initial conditions (bottom).

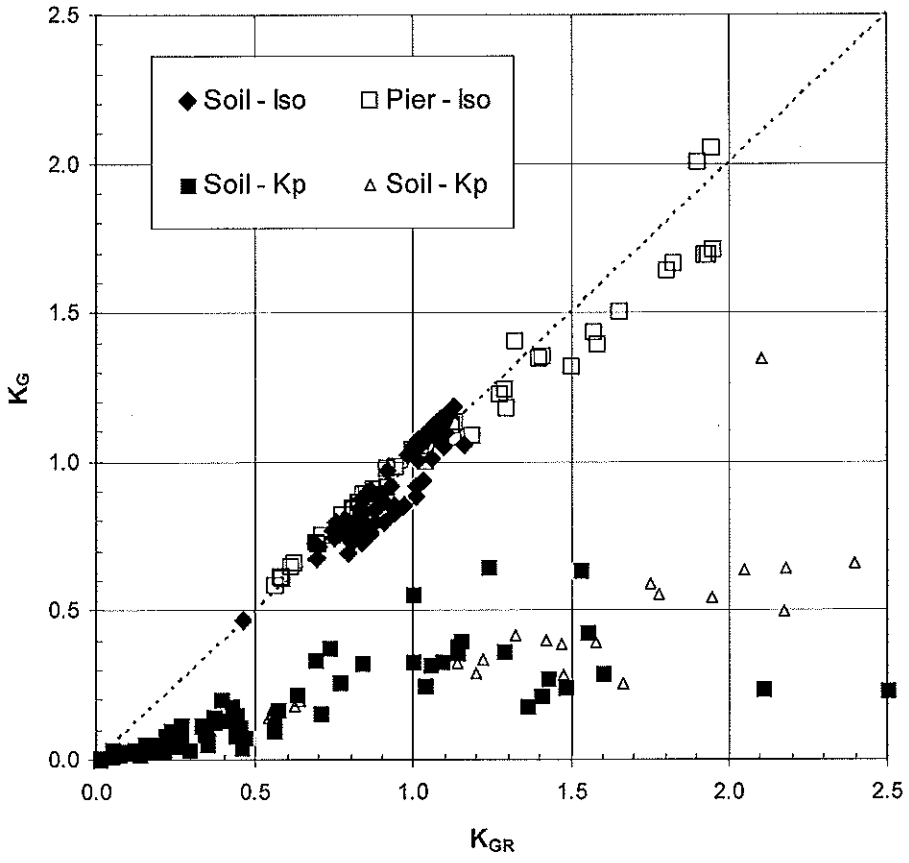

Figure 9 - Comparison of values of K_{GR} and K_G in the soil matrix and aggregate pier at various depths for Case C2, showing difference between K_p initial conditions and isotropic initial conditions.

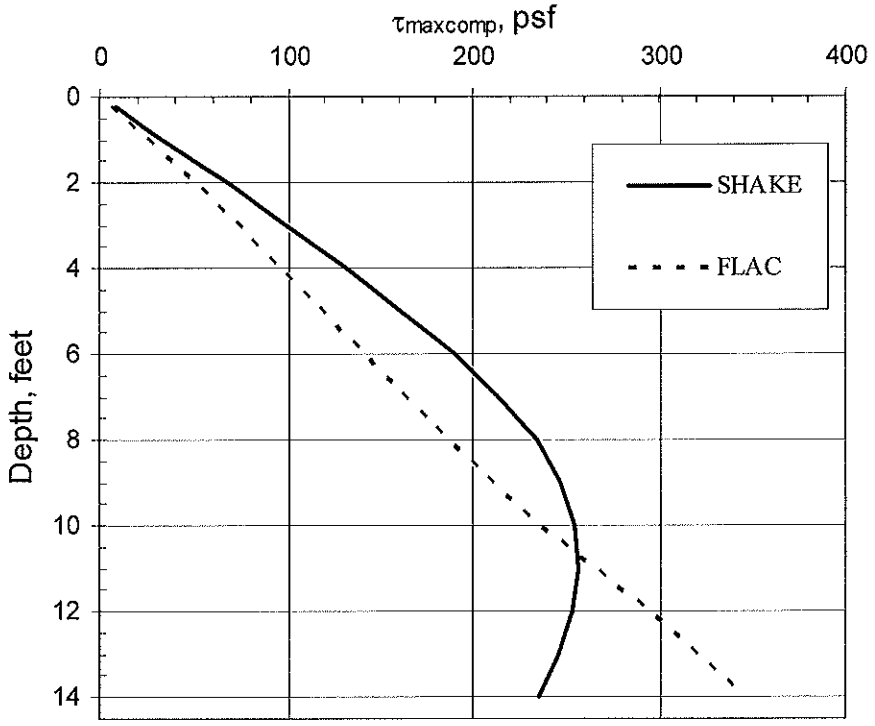

Figure 10 – Comparison between FLAC and composite SHAKE site response analyses for ground reinforced with the aggregate pier.

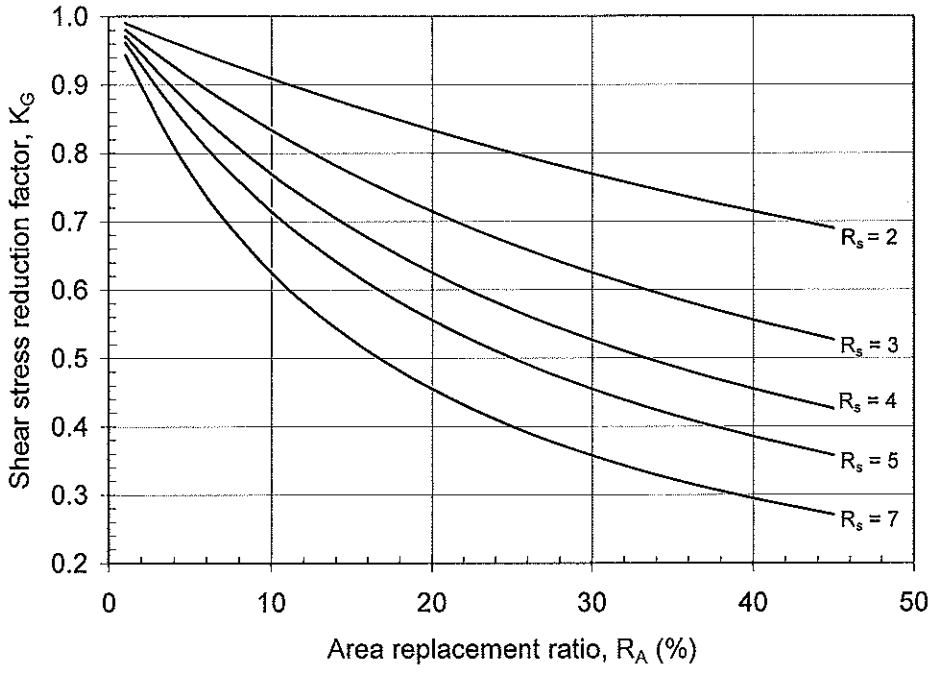

Figure 11 - The shear stress reduction factor, K_G (after Baez and Martin, 1993, 1994)

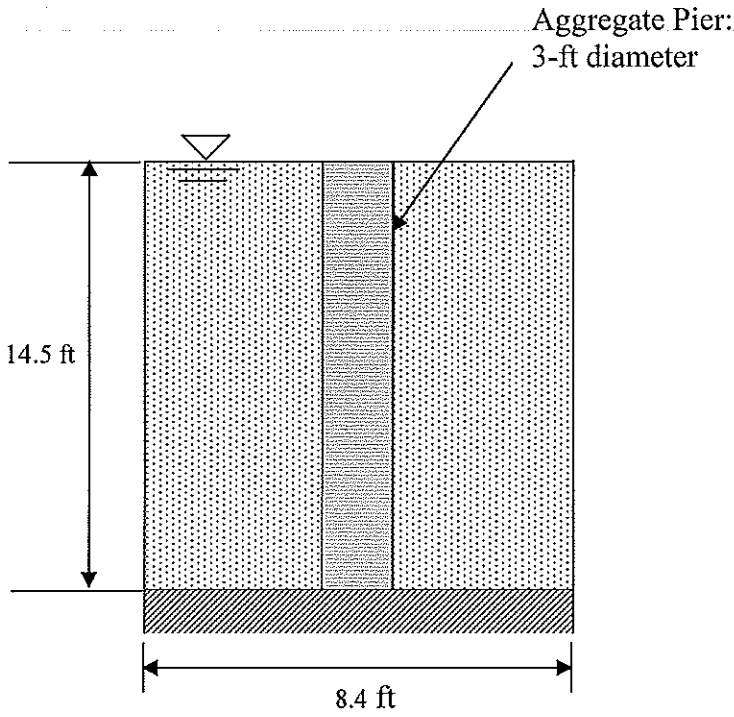

Figure 12 – Example problem geometry

Table 3 - Material properties and areas for example problem.

	Soil Matrix	Pier
γ_{sat}, pcf	120	147
G, psf	121000	968000
V_s, fps	180	460
A, ft^2	63.49	7.07